



Registration of Thoracic CT-CT Images Using Improved Demon Registration

Siti Salasiah Mokri ^{1*}, Ashrani Abd Rahni¹, Seri Mastura Mustaza¹, Norazreen Abd Aziz², Noraishikin Zulkarnain¹, Nasharuddin Zainal²

¹Pusat Kejuruteraan Sistem Bersepadu dan Teknologi Termaju (INTEGRA), Faculty of Engineering and Built Environment, 43600 Universiti Kebangsaan Malaysia, Selangor

²Centre of Advanced Electronic and Communication Engineering (PAKET), Faculty of Engineering and Built Environment, 43600 Universiti Kebangsaan Malaysia, Selangor

*Corresponding author E-mail: siti1950@ukm.edu.my

Abstract

Computed Tomography (CT) image is commonly used for medical diagnosis, to monitor disease progression as well in radiotherapy planning and treatment. In basis, image registration aims to accurately align two or more monomodal or multimodal images taken at different time or places. In order to accurately register two CT images, an accurate and reliable registration algorithm is required. This paper proposes an improved Demon registration technique that uses sum of conditional variance (SCV) and multi-modality independent neighborhood descriptive (MIND) similarity metrics instead of the conventional sum squared difference (SSD) demon method to register whole body CT (PET/CT) and thoracic CT images that are acquired separately. We tested our proposed method on 9 whole body CT (PET/CT) and CT images of Non-small Cell Lung Cancer (NSCLC). Apart from visual observation, the proposed method is compared with the free form deformation (FFD) and standard demon methods. The registration accuracy was justified by measuring the lung volumes overlap between the two images post registration in terms of the Jaccard and Dice coefficients. The quality of the registered images was measured using three image quality metrics; structural similarity index (SSIM), peak signal to noise ratio (PSNR) and correlation coefficient (CC). In overall, the performance of the proposed demon is double than FFD and is superior than the standard demon. The average Jaccard and Dice coefficients are 0.83 and 0.90 respectively. Results of SSIM, PSNR and CC metrics also indicate that the improved demon method is the best, followed by FFD and standard demon.

Keywords: CT Thoracic CT; demon registration; free form deformation; image registration; PET/CT; whole body;

1. Introduction

CT imaging is a of tomographic imaging that produces 2D/3D volumetric images of the anatomy. The technology is based on X-ray transmission where the patient is transmitted with X-rays generated from an X-ray tube, which are then detected by the detectors. The X-rays are attenuated at different levels depending on the types of body tissues resulting in anatomical based images. CT imaging plays an important role in medical applications especially in screening and diagnosing diseases at various parts of the body including the head, the lungs, the heart, the abdomen, the pelvic; etc. Particularly at the thoracic area, some of the diseases detected in CT images are acute and chronic changes in the lung parenchyma, tumour, emphysema and inflammation [1].

Image registration is the process of matching two images together by finding the optimal transformation through optimization [2]. Aligning two images is necessary when the images are taken at different times, at different places, have different perspectives or are coming from different image modalities. In medical applications, image registration is used in image-guided radiation therapy (IGRT), intensity-modulated radiation therapy (IMRT), image-based surgery, Magnetic Resonance Imaging (MRI) functional analysis, and tumour detection using state of the art medical imaging modalities. In general, image registration has also been applied in computer vision, pattern recognition, remote sensing, cartography, biometrics among others [3],[4].

Registration of the CT images at the thoracic area is used to monitor the progression of diseases; such as lung related diseases or the size/location of the tumours from time to time by comparing two or more CT images acquired at different times or probably different places [1]. Before any comparison and interpretation are made by the physician, these images need to be aligned/registered. Normally, image registration is conducted subjectively by manually registering the images. However, this approach is prone to inconsistency as the assessment may differ by one expert to another. In addition, registration of CT images is used in an online adaptive radiotherapy. In this routine, computed tomography CT image of the patient is taken for treatment planning before the patient undergoes radiotherapy treatment. Then cone beam CT [5] CBCT image is acquired before each treatment fraction to re-establish the previous treatment planning in order to compensate for any biological motions/changes of organs and tumours [6],[7], [8]. For this reason, the planning CT image needs to be registered to the daily CBCT image.

Therefore, finding the optimal transformation to accurately register the two images (CT-CT or CT-CBCT) can be achieved using compute- based image registration algorithms such as Demon and Free Form Deformation methods. This paper proposes an improved

demon registration method in registering CT images acquired at different times, in specific, that is in registering whole body CT (PET/CT) to thoracic CT image. [6] applied a variant of demon registration called Deformation with Intensity Simultaneously Corrected (DISC) wherein an adaptive intensity correction step was executed in every iteration to register CT-CBCT. On the other hand, [7] performed feature-based demon registration method in which prior delineated structures were integrated into the original Demon through the energy function. Instead, this paper proposes a new variant of Demon registration method that is based on Modality Independent Neighbourhood Descriptor (MIND) and Sum of Conditional Variance (SCV) similarity measures instead of the original sum squared difference (SSD) based Demon method to register whole body CT (PET/CT) to thoracic CT images.

2. Methodology

The basis of the classical demon registration by [9] is the optical flow transformation model in which the image m is diffused to match the reference image f by finding the optimum displacement fields, D_a . The displacement field, D_a is found by minimising the demon energy function E_{demon} defined as:

$$E_{demon} = \frac{1}{\sigma_i^2} \|f - m\Delta D_a\|^2 + \frac{1}{\sigma_T^2} \text{Re } g(D_a) \quad (1)$$

where $\|f - m\Delta D_a\|^2$ is the sum squared difference (SSD) between the moved image $m\Delta D_a$ and the reference image f while $\text{Re } g(D_a)$ is the regularisation of D_a . It is the uncertainty weight, and parameters σ_i and σ_T are the intensity and the displacement fields', respectively. The displacement field is iteratively updated in every voxel X as follows (Note: ∇m is the gradient of m)

$$D_u(X) = \frac{(f(X) - m(X) \times \nabla m)}{(f(X) - m(X))^2 + \|\nabla m\|^2} \quad (2)$$

There are several variants of demon technique that have been proposed thus far ([10],[11],[12]). In specific, [12] added a transformation error function together with the SSD and the deformation field regularisation terms in the demon energy computation as follows:

$$E_{demon} = \frac{1}{\sigma_i^2} \|f - m\Delta D_c\|^2 + \frac{1}{\sigma_x^2} \text{dist}(D_a, D_c) + \frac{1}{\sigma_T^2} \text{Re } g(D_a) \quad (3)$$

Here, D_c is known as correspondence field and σ_x is the spatial uncertainty weight between D_a and D_c . Two steps optimisation are used to solve the newly defined demon energy in (3) by dividing this equation into two as the following:

$$\frac{1}{\sigma_i^2} \|f - m\Delta D_c\|^2 + \frac{1}{\sigma_x^2} \text{dist}(D_a, D_c) \quad (4)$$

and

$$\frac{1}{\sigma_x^2} \text{dist}(D_a, D_c) + \frac{1}{\sigma_T^2} \text{Re } g(D_a) \quad (5)$$

(4) and (5) are solved by calculating D_u and performing Gaussian filter on D_a respectively.

It was suggested in [13] to replace the SSD based term in the classical demon energy function with sum of conditional variances (SCV) similarity measure introduced by [14] to attune the monomodal functionality in solving multimodal registration problem. In this paper, we propose to combine the SCV with Modality Independent Neighbourhood Descriptor (MIND) by [15] to further improve the robustness of the technique on many types of images. Although the strategy is initially aimed to expand the applicability of the standard demon registration technique on multimodal registration issue, we investigate the efficacy of our method as compared to the original demon on monomodal image registration problem in particular to CT-CT registration. We anticipate that, generally, the proposed method generates better registration performance than its original as well as the establish free form deformation (FFD) method for CT-CT image datasets.

By definition, sum of conditional variance (SCV) between the reference image f with pixel values f_i and the moving image m with pixel values m_i at a particular iteration can be computed as:

$$SCV = \sum_{i=1}^N E\left([f_i - E(f_i | m_i)]^2 | m_i \in \Delta_j\right) \quad (6)$$

where N is the number of pixels in the image, $E(\cdot)$ is the expectation operator and Δ_j is a set of histogram bin of m_i . (6) can be rewritten as:

$$SCV = \sum_{i=1}^N (f_i - \hat{m}_i)^2 \quad (7)$$

$$\hat{m}_i = E(f_i | m_i \in \Delta_j) \quad (8)$$

\hat{m}_i is calculated based on the statistical association (joint probability distribution) of m and f . On the other hand, Modality Independent Neighbourhood Descriptor (MIND) extracts the structure similarity between both images to guide the registration process. To obtain the MIND descriptor for image f , the intensity distance function D_p between the two pixels X_1 and X_2 is calculated as follows:

$$D_p(f, X_1, X_2) = \sum_{p \in \Pi} ((f(X_1 + p) - f(X_2 + p))) \quad (9)$$

Where $D_p(f, X_1, X_2)$ is the sum squared intensity differences between two groups of pixels contained within two patches p that are positioned at X_1 and X_2 of the image f . Then, MIND descriptor for image f at a pixel X_c with a given neighbour r is defined as:

$$MIND(f, X_c, r) = \frac{1}{n} (\exp(-\frac{D_p(f, X_c, X_c + r)}{V(f, X_c)})), r \in R \quad (10)$$

where

$$V(f, X_c) = \frac{1}{4} \sum_k D_p(f, X_c, X_c + k) \quad (11)$$

$V(f, X_c)$ is the mean of the intensity distance of pixel X_c within a four neighbourhood. The parameter R defines a search region and n is a normalisation constant. Finally, the similarity metric based on MIND between the two images f and m is defined as:

$$S_{MIND}(X) = \frac{1}{|R|} \sum_{r \in R} |MIND(f, X, r) - MIND(m, X, r)| \quad (12)$$

We suggest utilising SCV and MIND based similarity measures in the definition of the deformation update field D_u as follows:

$$D_u(X) = k_{SCV} \sigma_{SCV} D_{SCV}(X) + k_{MIND} \sigma_{MIND} D_{MIND}(X) \quad (13)$$

where k_{SCV} and k_{MIND} are the weighting factors of SCV and MIND respectively, while σ_{SCV} and σ_{MIND} represent the iteration steps. Mokri et al., (2015), proposed to update the deformation field term of SCV as in (14),

$$D_{SCV}(X) = \frac{(f(X) - m(X)) \times \nabla \hat{m}}{\|\nabla \hat{m}\|^2 + \frac{\sigma_i^2}{\sigma_x^2}} \quad (14)$$

in which the number of histogram bin needed to calculate \hat{m} must be defined. Here, we propose to adapt MIND similarity measure in which the following energy function is used:

$$S = \sum_{i=1}^N S_{MIND}((f(X), m) \Delta D_a(X))^2 \quad (15)$$

The updated deformation field of S_{MIND} is formulated as:

$$D_{MIND} = -S_{MIND} \nabla S_{MIND}(D_a) \quad (16)$$

where $\nabla S_{MIND}(D_a)$ is the gradient of S_{MIND} with respect to the deformation field D_a .

Overall, the algorithm is as follows:

1. Iterate until convergence
2. Compute the displacement update field using:

$$u(X) = \frac{(f(X) - m(X)) \times \nabla m}{\|\nabla m\|^2 + \frac{\sigma_i^2}{\sigma_x^2}} \quad (17)$$

3. Regularise the update field with Gaussian smoothing as $D_u = \psi_{fluid}(D_u)$. ψ_{fluid} is the Gaussian smoothing process where the Gaussian width is defined as σ_{fluid} .
4. Calculate the current D_a by adding the current D_u with the previous D_a through an addition of $D_a = \phi(D_a, D_u) = D_a + D_u$.

5. Regularise the current D_a with Gaussian smoothing, $D_a = \psi_{diff}(D_a) \cdot \psi_{diff}$ is the Gaussian smoothing process where the Gaussian width is defined as σ_{diff} .
6. Warp the moving image according $m_{warp} = m\Delta D_a$.

2.1 Experimental study

The proposed hybrid demon registration was tested on CT images archived from the “Non-small Cell Lung Cancer (NSCLC) Radiogenomics: Initial Stanford Study of 26 Cases” database [16]. Nine patient datasets were used in the experiment in which each dataset contains one whole body PET/CT images and one thoracic CT image. In most of the datasets, the thoracic CT images were scanned before the PET/CT acquisition within an interval of several days up to few months.

In our study, the whole body CT image (PET/CT) was moved to the thoracic CT image. First, we cropped the thoracic region in both types of images and resampled the whole body image to match the size of the fixed image. Then, we rigidly registered the body region in the moving image to the corresponding body region of the fixed image. For the purpose of body registration, the body regions in both CT images were segmented using thresholding, morphological processes and 3D connected labelling [17].

2.2 Validation

The performance of the proposed hybrid demon registration was evaluated quantitatively and qualitatively. Qualitative evaluation was based on the improvement of the registration as seen visually while the quantitatively evaluation was made by considering the lung volume overlap from both moving and fixed CT images before and after the registration process. To obtain the lung volume, the lungs were segmented according to [17] before and after the registration process. Two volume overlap criteria were used for this reason namely the Jaccard and Dice coefficients which numbers are ranged between 0 to 1. The value of 1 indicates perfect overlap (perfect registration) while 0 indicates no overlap (total misregistration). The Dice and Jaccard coefficients measure the spatial overlap between two volumes, in which the values are in the range of 0 (no overlap) and 1 (perfect overlap). These measures are quantified based on the following [18]:

$$Jaccard = \frac{A \cap M}{A \cup M} \quad (18)$$

$$Dice = \frac{2(A \cap M)}{(A \cap M) + (A \cup M)} \quad (19)$$

In addition to the Dice and Jaccard coefficients, the registration achievement post registration was observed by comparing the quality of the registered moving CT image in reference to the fixed CT image in terms of three image quality metrics; structural similarity index (SSIM), peak signal to noise ratio (PSNR) and correlation coefficient (CC) ([19][20][21]) Generally, SSIM [22] measures the similarity between two images through the assessment of luminance, contrast and structure in both images, and its value is between 0-1. SSIM of 1 implies that both the moving and reference are fully correlated while 0 means that there is no correlation between the two images. SSIM between two images x and y is calculated according to:

$$SSIM(x, y) = [I(x, y)] [c(x, y)] [s(x, y)] \quad (20)$$

$$I(x, y) = \frac{2\mu_x \mu_y + C_1}{\mu_x^2 + \mu_y^2 + C_1}$$

$$c(x, y) = \frac{2\sigma_x \sigma_y + C_2}{\sigma_x^2 + \sigma_y^2 + C_2}$$

$$s(x, y) = \frac{\sigma_{xy} + C_3}{\sigma_x \sigma_y + C_3}$$

and $\mu_x, \mu_y, \sigma_x, \sigma_y, \sigma_{xy}$ are the averages, standard deviations and covariance between the two images while C_1, C_2 and C_3 are three variables to stabilize denominator in each term in (20). Peak signal noise ratio (PSNR) is calculated based on the mean squared error between the two images, x and y according to the number of columns, rows and slices of the images, M, N, O as follows:

$$MSE = \frac{\sum_{MNO} [x_{MNO} - y_{MNO}]^2}{M * N * O} \quad (21)$$

$$PSNR = 10 \log_{10} \left(\frac{R^2}{MSE} \right) \quad (22)$$

where R is the maximum value of the image. On the other hand, correlation coefficient (CC) is calculated as:

$$CC = \frac{\sum_M \sum_N \sum_O (x_{MNO} - \bar{x})(y_{MNO} - \bar{y})}{\sqrt{(\sum_M \sum_N \sum_O (x_{MNO} - \bar{x})^2)(\sum_M \sum_N \sum_O (y_{MNO} - \bar{y})^2)}} \quad (23)$$

where \bar{x} and \bar{y} are the averages of both images, respectively.

3. Experimental results

We quantitatively evaluated the registration results by comparing our proposed demon with SSD demon and free form deformation (FFD) methods in terms of Jaccard and Dice coefficients as well as structural similarity index (SSIM), peak signal to noise ratio (PSNR) and correlation coefficient (CC). In order to equally compare the efficiency of the proposed method and the SSD original demon methods, we defined similar number of iteration and multiresolution for both.

Table 1 presents the Jaccard coefficient results post registration for the three methods of nine CT-CT datasets. The Jaccard coefficient values obtained after the body to body rigid registration between the two images are also presented. On average, registering the body region through rigid registration increased the Jaccard average value by an almost 150% (0.69 from 0.28). This step is necessary to match the scale of the moving image's body to the fixed image's body.

Thereafter, the performance of the three methods is made by calculating the percentage increment of their Jaccard values with respect to the value achieved after body to body registration process, marked as % in Table 1. The table shows that the improvement acquired using the proposed demon method is approximately two times higher than FFD (21.12% vs 12.94%) and is greatly better than the standard SSD demon method.

The dice coefficient results in Table 2 also show the similar outcome. In obvious, the misregistration of the tested thoracic CT and whole body CT images before the registration is very significant in which the Jaccard and Dice values pre-registration are 0.28 and 0.43 respectively.

Table 3 presents the results of structural similarity index (SSIM), peak signal to noise ratio (PSNR) and correlation coefficient (CC) values that signify the quality of the image post registration. In overall, the proposed demon generates the best image quality results for all the datasets. These values indicate that, among the three, the proposed demon is the best, followed by FFD and finally the standard SSD demon techniques.

Figure 1 – 9 illustrate the registration using the proposed demon method of the nine CT datasets prefixed by GSMXXXXXX. Each figure consists of the whole-body CT (PET/CT) as fixed CT, the thoracic CT as floating/moving image and the registered thoracic CT as the result of the registration process. It is evident that the size of the patient body in the entire floating images is smaller than in the fixed image. Therefore, initial global, rigid registration particularly in matching the scale of the floating image to the fixed image is necessary to compensate this. All figures show that our improved demon method that works at the local scale has successfully registered the moving image to the corresponding fixed image satisfactorily as seen from the axial (top), sagittal (middle) and coronal (bottom) views.

Our results show that the proposed method has better performance than the conventional SSD especially in tackling the whole-body CT (PET/CT) and thoracic CT misregistration problem. As both images are taken at different time, which interval may take several days or few months, using sum squared difference (SSD) that based on the intensity similarity between the two images is incompetent. This is because the progression of the disease inflicting the patients' thoracic area may change the morphology in the area. For instance, the size and the location of the tumour may change along the interval of the two separate acquisitions. The uses of Modality Independent Neighbourhood Descriptor (MIND) and Sum of Conditional Variance (SCV) consider the structure similarity and the statistical relationship between the two images, thus bringing robustness in the proposed method to generally solve two monomodal images that bear morphological difference as well as unexpected changes of the disease across time.

Table 1: Comparison of Jaccard coefficient pre and post registration

Patient ID	Jaccard							
	Before	Body to body registration	FFD	%	Standard demon	%	Proposed demon	%
GSM714046	0.3622	0.8461	0.8665	2.41	0.8123	-3.99	0.8951	5.79
GSM714047	0.3296	0.5867	0.7461	27.16	0.6092	3.83	0.7605	29.62
GSM714050	0.4490	0.8078	0.8438	4.45	0.6069	-24.87	0.8555	5.90
GSM714056	0.1741	0.5309	0.5950	12.07	0.5155	-2.90	0.6547	23.31
GSM714057	0.1142	0.6208	0.7557	21.73	0.4807	-22.56	0.8472	36.46
GSM714058	0.1756	0.8354	0.8457	1.23	0.8984	7.54	0.9031	8.10
GSM714060	0.3000	0.6126	0.6846	11.75	0.6604	7.80	0.8049	31.39
GSM714061	0.4181	0.6109	0.7945	30.05	0.7956	30.23	0.8045	31.69
GSM714068	0.2309	0.7147	0.7551	5.65	0.8002	11.96	0.8424	17.86
Average	0.28	0.68	0.77	12.94	0.69	0.78	0.82	21.12

Table 2: Comparison of Dice coefficient pre and post registration

Patient ID	Dice							
	Before	Body to body registration	FFD	%	Standard demon	%	Proposed demon	%
GSM714046	0.5318	0.9166	0.9258	1.00	0.8946	-2.40	0.9446	3.05
GSM714047	0.4958	0.7395	0.8546	15.56	0.7572	2.39	0.8640	16.83
GSM714050	0.6198	0.8937	0.9153	2.41	0.9221	3.17	0.9512	6.433
GSM714056	0.2965	0.6936	0.7461	7.56	0.6803	-1.91	0.7913	14.08
GSM714057	0.2050	0.7660	0.8608	12.37	0.6943	-9.36	0.9173	19.75
GSM714058	0.2987	0.9103	0.9164	0.67	0.9185	0.90	0.9491	4.26
GSM714060	0.4615	0.7598	0.8128	6.97	0.7955	4.69	0.8919	17.38
GSM714061	0.5987	0.7584	0.8568	12.97	0.8861	16.83	0.8988	18.5
GSM714068	0.3752	0.8336	0.8605	3.22	0.8599	3.15	0.9144	9.69
Average	0.43	0.81	0.86	6.97	0.8231	1.94	0.90	12.22

Table 3: Comparison of SSIM, cross correlation (CC) and peak SNR post registration

Patient ID	MI			Standard Demon			Proposed Demon		
	SSIM	CC	P-SNR	SSIM	CC	P-SNR	SSIM	CC	P-SNR
GSM714046	0.7349	0.9827	23.47	0.7499	0.9190	24.25	0.7896	0.9927	24.35
GSM714047	0.6321	0.9647	19.75	0.6007	0.9692	21.10	0.7986	0.9927	24.32
GSM714050	0.6145	0.9397	15.85	0.6048	0.9497	16.38	0.7060	0.9613	16.57
GSM714056	0.5183	0.8086	13.74	0.5002	0.7353	13.33	0.5561	0.8360	14.02
GSM714057	0.4007	0.8500	16.40	0.2860	0.6796	11.64	0.4429	0.8793	17.16
GSM714058	0.6711	0.9774	24.07	0.6348	0.9718	23.84	0.7388	0.9881	24.43
GSM714060	0.6708	0.9854	21.39	0.6615	0.9765	21.13	0.7378	0.9911	21.44
GSM714061	0.6679	0.9812	21.50	0.6701	0.9835	21.78	0.7288	0.9880	21.91
GSM714068	0.8577	0.9863	24.85	0.8072	0.9714	24.67	0.8997	0.9942	25.31
Average	0.6408	0.9417	20.11	0.6128	0.9062	19.79	0.7109	0.9581	21.05

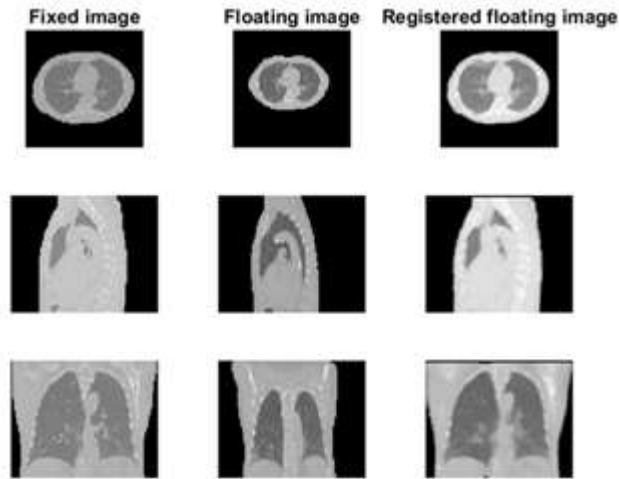


Fig1: Registration results for GSM714046

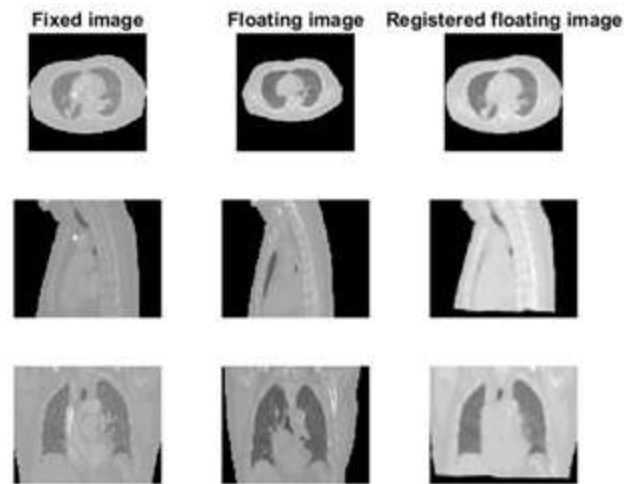


Fig2: Registration results for GSM714047

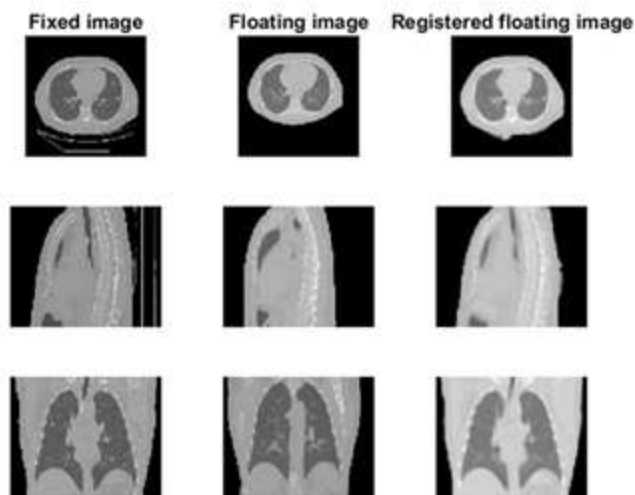


Fig3: Registration results for GSM714050

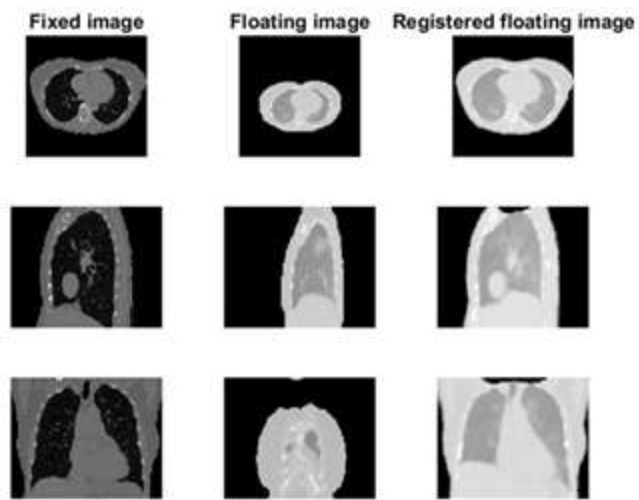


Fig4: Registration results for GSM714056

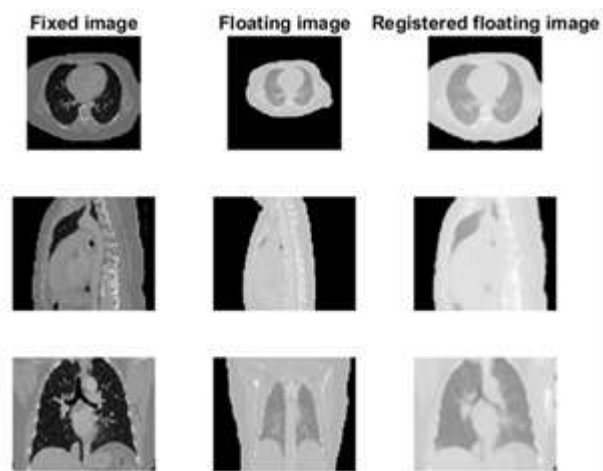


Fig5: Registration results for GSM714057

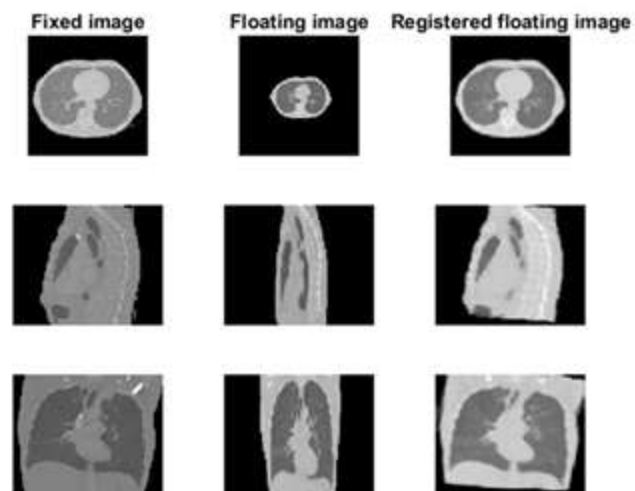


Fig6: Registration results for GSM714058

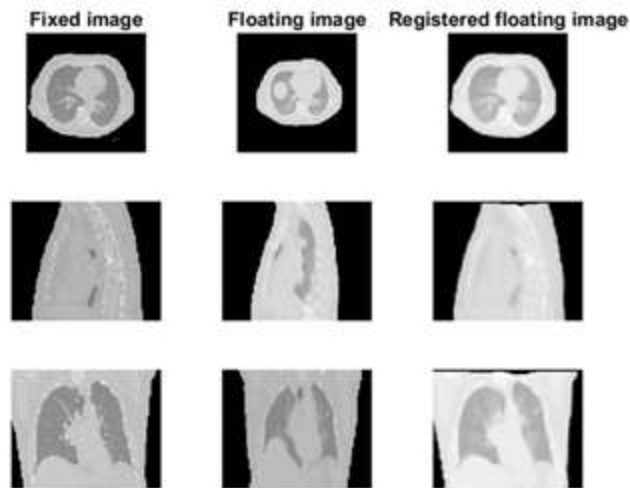


Fig7: Registration results for GSM714060

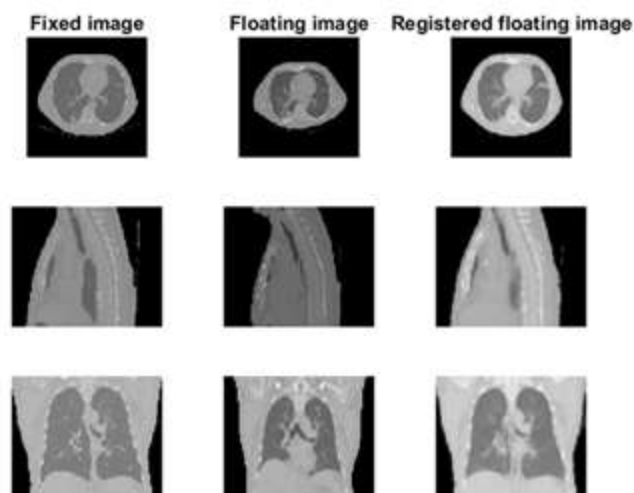


Fig8: Registration results for GSM714061

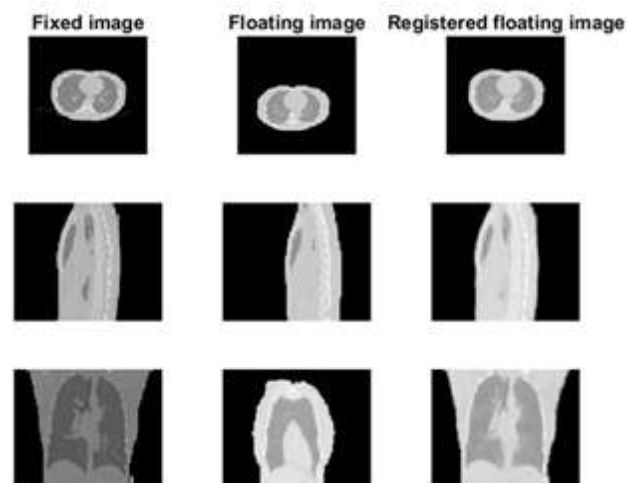


Fig9: Registration results for GSM714068

4. Conclusion

This paper proposes an improved demon registration method using a combination of SCV and MIND based similarity measures applied on whole body CT and CT of PET/CT registration problem separated by time. Experimentation on Non-small Cell Lung Cancer (NSCLC) Radiogenomics: Initial Stanford Study of 26 Cases⁷ database generates better registration accuracy as compared to the original SSD based demon and free form deformation (FFD) registration methods in terms of visual assessment as well as quantitative evaluation based on lung overlap volume and several image quality parameters; SSIM, CC and peak SNR (PSNR). In case of lung volume overlap post registration, our proposed method generates better Jaccard and Dice achievements which are double than the FFD method and exceptionally better than the original Demon post registration. Correspondingly, the results of the three different image quality metrics show that our proposed modified demon method is superior than FFD and SSD based demon registration techniques.

Acknowledgement

The authors would like to acknowledge Faculty of Engineering and Built Environment and Universiti Kebangsaan Malaysia for the facilities and financial supports through research grant code number GGPM-2017-069.

References

- [1] Gorbunova V, Spurring J, Lo P, Loeve M, Tiddens HA, Nielsen M & de Bruijne M (2012), Mass preserving image registration for lung CT. *Medical image analysis*, 16(4), 786-795.
- [2] Oliveira FPM & Tavares JMRS (2014), Medical image registration: a review. *Computer Methods Methods in Biomechanics and Biomedical Engineering*, 17.2, 73-93.
- [3] Zitova B & Flusser J (2003), Image registration methods: a survey, *Image Vision Computing*, 21, 977-1000.
- [4] Xiong Z & Zhang YA (2010), A critical review of image registration methods. *International Journal of Image and Data Fusion*, 1, 137-158.
- [5] Amin AM & Rahni AA (2017), Modelling the Siemens SOMATOM Sensation 64 Multi-Slice CT (MSCT) Scanner. *Journal of Physics: Conference Series*, 851, 012012.
- [6] Zhen X, Gu X, Yan H, Zhou L, Jia X & Jiang SB (2012), CT to cone-beam CT deformable registration with simultaneous intensity correction. *Physics in Medicine & Biology*, 57(21),6807.
- [7] Wu Q, Cao R, Pei X, Jia J & Hu L (2015), Deformable image registration of CT images for automatic contour propagation in radiation therapy. *Bio-medical materials and engineering*, 26(s1), S1037-S1044.
- [8] Nielsen MS, Østergaard LR & Carl J (2015), A new method to validate thoracic CT-CT deformable image registration using auto-segmented 3D anatomical landmarks. *Acta Oncologica*, 54(9), 1515-1520.
- [9] Thirion JP (1995), Fast Non-Rigid Matching of 3D Medical Images, Technical Report 2547. Institut National de Recherche en Informatique et en Automatique, 37.
- [10] Pennec X, Cachier P & Ayache N, Understanding the “demon’s algorithm”: 3D non-rigid registration by gradient descent, In *International Conference on Medical Image Computing and Computer-Assisted Intervention*, (1999), 597-605.
- [11] Vercauteren T, Pennec X, Perchant A & Ayache N (2009), Diffeomorphic demons: efficient non-parametric image registration. *NeuroImage*, 45, S61–72.
- [12] Cachier P, Bardinet E, Dormont D, Pennec X, & Ayache N (2003), Iconic feature based nonrigid registration: The PASHA algorithm. *Computer Vision Image Understanding*, 89(2), 272-298.
- [13] Mokri SS, Saripan MI, Marhaban MH, Nordin AJ & Hashim S (2015), Hybrid registration of PET/CT in thoracic region with pre-filtering PET sinogram. *Radiation Physics and Chemistry*, 116, 300-304.
- [14] Pickering MR, Muhit AA, Scarvell JM & Smith PN, A new multi-modal similarity measure for fast gradient-based 2D-3D image registration, in *Proceedings of International Conference of the IEEE Engineering in Medicine and Biology Society*, (2009), 5821–4.
- [15] Heinrich MP, Jenkinson M, Bhushan M, Matin T, Gleeso FV, Brady SM & Schnabel JA (2012), MIND: modality independent neighbourhood descriptor for multi-modal deformable registration. *Medical Image Analysis*,16,1423–1435.
- [16] Napel S & Plevritis SK, “NSCLC Radiogenomics: Initial Stanford Study of 26 Cases”, *The Cancer Imaging Archive*. (2014), <http://doi.org/10.7937/K9/TCIA.2014.X7ONY6B1>
- [17] Mokri SS, Saripan MI, Marhaban MH & Nordin AJ, “Lung segmentation in CT for thoracic PET-CT registration through visual study”, *Biomedical Engineering and Sciences (IECBES)*, *IEEE EMBS Conference on*, (2012), 550-554.
- [18] Yang F & Grigsby PW (2012), Delineation of FDG-PET tumors from heterogeneous background using spectral clustering. *European Journal of Radiology*, 81(11), 3535–41.
- [19] Kher HR (2014), Implementation of image registration for satellite images using mutual information and particle swarm optimization techniques. *International Journal of Computer Applications*, 97(1), 7-14.
- [20] Zhang X, Gilliam C & Blu T, “Iterative fitting after elastic registration: An efficient strategy for accurate estimation of parametric deformations”, *IEEE Conference in Image Processing (ICIP)*, (2007), 492-1496.
- [21] Pradhan S & Patra D (2016), Enhanced mutual information based medical image registration. *IET Image Processing*, 10(5), 418-427.
- [22] Wang Z, Bovik AC, Sheikh HR & Simoncelli EP (2004), Image quality assessment: from error visibility to structural similarity. *IEEE transactions on image processing*, 13(4), 600-612.